Supporting information for:

^{35}Cl Dynamic Nuclear Polarization Solid-State NMR of Active Pharmaceutical Ingredients

David A. Hirsh,[1] Aaron J. Rossini,[2,3*] Lyndon Emsley,[4] and Robert W. Schurko[1*]

[1]*Department of Chemistry & Biochemistry, University of Windsor, Windsor, ON, Canada N9B 3P4*
[2]*Department of Chemistry, Iowa State University, Ames, IA, USA 50011-3111*
[3]*US DOE Ames Laboratory, Ames, Iowa 50011*
[4]*Institut des Sciences et Ingénierie Chimiques, Ecole Polytechnique Fédérale de Lausanne (EPFL), Lausanne, Switzerland CH-1015*
[*]*Authors to whom correspondence should be addressed:*
A.J.R. Phone: 515-294-8952, E-mail: arossini@iastate.edu
R.W.S. Phone: 519-253-3000 x3548 E-mail: rschurko@uwindsor.ca

Supporting Information Provided:

Table S1. Sample characteristics, measured DNP enhancements, and relaxation properties.

sample name and composition of the impregnating liquid	brand name/retailer	ε_C(CP)	ε_{Cl}(CP)	T_{DNP}(^{1}H) /s	^{13}C Sensitivity	recycle delay [/s][b]
Hist (15 mM TEKPol, TCE)	Sigma-Aldrich	260	50	302	22.2	30
Ambr (15 mM TEKPol, TCE)	Sigma-Aldrich	92	15	28	38.0	30
Diph (15mM TEKPol, 1,3-dibromobutane)	Sigma-Aldrich	25	6	3	0.7	22
Diph Dosage (15mM TEKPol, 1,3-dibromobutane)	Life Brand (25 mg)	16	–[a]	16.9	0.5	22
Isox (15 mM TEKPol, TCE)	Sigma-Aldrich	86	12	14.7	8.0	20
Isox Dosage (15 mM TEKPol, TCE)	Prevention Labs (10 mg)	12	–[a]	13.8	2.3	20
Ceti (15 mM TEKPol, 1,3-dibromobutane)	Sigma-Aldrich	20	5.8	14.1	8.7	10
Cetirizine HCl Dosage (15 mM TEKPol, 1,3-dibromobutane)	Reactine (10 mg)	8	2.6	12	8.2	10

[a]e_{Cl}(CP) is not measurable for these dosage forms as the MW off spectra would require excessive experimental time.
[b]The optimized recycle delay of 1.3 × T_1(^{1}H) was used for both ^{13}C and ^{35}Cl experiments.

Table S2. Weight percentage of chlorine in the samples, and wt-% of API in dosage forms.

sample name	composition of the impregnating liquid	API wt-%[a]	Cl wt-%[b]
Hist	15 mM TEKPol, TCE	98	18.31
Ambr	15 mM TEKPol, TCE	99	8.38
Isox	15 mM TEKPol, TCE	98	10.3
Isox Dosage	15 mM TEKPol, TCE	4.95	0.52
Diph	15 mM TEKPol, 1,3-dibromobutane	98	11.9
Diph Dosage	15 mM TEKPol, 1,3-dibromobutane	6.12	0.74
Ceti	15 mM TEKPol, 1,3-dibromobutane	98	7.52
Ceti Dosage	15 mM TEKPol, 1,3-dibromobutane	5.78	0.45

[a]The percent weight of the active ingredient within the bulk form (*i.e.*, purity) was indicated by Sigma-Aldrich upon purchase.

The percent weight of the active ingredient within the dosage form was calculated as follows:

$$\%\ \text{weight of API} = \frac{\text{Dose of active ingredient}}{\text{Tablet weight}} \times 100\ \%$$

[b]The percent weight of Cl within the bulk form was calculated as follows:

$$\%\ \text{weight of Cl} = \frac{\text{moles Cl}}{\text{moles API}} \times \frac{\text{MW of Cl}}{\text{MW of API}} \times \text{purity of sample} \times 100\ \%$$

The percent weight of the Cl within the dosage form was calculated as follows:

$$\%\ \text{weight of Cl} = \left[\frac{\left(\frac{\text{Stoichiometric MW of Cl in API}}{\text{MW of API}}\right) \times \text{Dose of API}}{\text{Tablet mass}}\right] \times 100\ \%$$

Table S3. Acquisition parameters for ^{1}H-^{13}C CP/MAS SSNMR experiments.

		Hist	Ambr	Isox		Diph		Ceti	
		Bulk	Bulk	Bulk	Dosage	Bulk	Dosage	Bulk	Dosage
Number of scans	MW on	4	4	8	64	32	4	8	8
	MW off	4	4	8	256	64	16	8	8
Experimental time (min)	MW on	2.0	2.0	2.4	19.2	2.1	1.5	1.3	1.3
	MW off	2.0	2.0	2.4	76.8	4.3	5.9	1.3	1.3
Recycle delay (s)		30	30	18	18	4	22	10	10
Spinning speed (kHz)		8	8	9	9	8	8	8	8
^{1}H 90° pulse width [π/2] (μs)		2.8	2.5	2.5	2.5	2.5	2.5	2.5	2.5
Contact time (ms)		2	2	2	2	2	2	2	2
^{1}H rf field during contact pulse (kHz)		100	100	100	100	100	100	100	100
^{13}C rf field during contact pulse (kHz)		71	71	71	71	71	71	71	71
^{1}H decoupling field (kHz)		90	90	90	90	90	90	90	90
Spectral width (kHz)		59.5	59.5	59.5	59.5	59.5	59.5	59.5	59.5
Acquisition length (number of points)		3802	3802	3802	2970	2048	3802	3802	3802

Table S4. Acquisition parameters for ^{13}C-^{35}Cl D-HMQC-R^3/MAS SSNMR experiments.

Spinning frequency (kHz)	8
Number of scans per t1 increment	8
Number of t1 increment	256
Recycle delay (s)	25
t1 increment (μs)	62.5
Spectral width in F2 (kHz)	25
Spectral width in F1 (kHz)	16
Acquisition length (number of points in F2)	1500
^1H 90° pulse width [π/2] (μs)	2.5
^{13}C 90° pulse width [π/2] (μs)	3.0
^{35}Cl 90° pulse width [π/2] (μs)	3.1
^{13}C R3 recoupling power (kHz)	9.6
Contact pulse length (ms)	2
^1H rf field during contact pulse (kHz)	80
^{13}C rf field during contact pulse (kHz)	40
^1H rf field during decoupling (kHz)	100

Table S5. Acquisition parameters for ^1H-^{35}Cl CP SSNMR experiments on **hist**.

		CP-CPMG	CP-echo (slow MAS)	CP-echo MAS
Number of scans	MW on	4	4	4
	MW off	8	4	16
Experimental time (min)	MW on	2.5	0.7	4
	MW off	5	0.7	16
Spinning speed (Hz)		0	250	8000
Recycle delay (s)		30	10	60
Spectral Width (kHz)		100	100	50
^1H π/2 pulse width (μs)		2.5	2.8	2.5
Contact time (ms)		6	6	9
^1H rf field during contact pulse (kHz)		70.7	70.7	50
^{35}Cl rf field during contact pulse (kHz)		51	51	18
^1H decoupling field (kHz)		87	100	50
Acquisition length (number of points)		13400	512	800
Meiboom-Gill loops [N] (*i.e.*, Number of echoes)		30	-	-
Refocusing pulse width (μs)		6.6	-	-

Table S6. Acquisition parameters for ^{1}H-^{35}Cl BCP SSNMR experiments.

	Ambr	Isox		Diph		Ceti	
	Bulk	Bulk	Dosage	Bulk	Dosage	Bulk	Dosage
Number of scans	16	16	3200	512	1024	32	2048
Experimental time (h)	0.3	0.1	16.0	3.1	6.3	0.2	10.2
Recycle delay (s)	30	20	18	22	22	18	18
Spectral Width (kHz)	500	500	500	500	500	500	500
^{1}H 90° pulse width [π/2] (μs)	2.5	2.5	2.5	2.5	2.5	2.5	2.5
Contact time (ms)	15	8	8	8	8	25	25
^{1}H Hartmann-Hahn matching field (kHz)	75	75	75	75	75	75	75
^{35}Cl Hartmann-Hahn matching field (kHz)	69	69	69	69	69	69	69
^{1}H decoupling field (kHz)	95	95	95	95	95	95	95
Meiboom-Gill loops [N] (*i.e.*, Number of echoes)	250	250	160	50	50	200	200
Acquisition length (number of points)	75250	75250	48250	15270	15270	60250	60250
Refocusing pulse width (μs)	25	25	25	25	25	25	25
Sweep range of refocusing pulses (kHz)	250	250	250	250	250	250	250
Sweep range of ^{35}Cl contact pulse (μs)	250	200	250	150	150	250	250

Table S7. Experimental ^{35}Cl EFG tensor parameters for HCl salts.[a]

sample name		C_Q (MHz)[b]	η_Q[c]	δ_{iso} (ppm)[d]	Ω (ppm)[e,h]	κ[f,h]	α (°)[g,h]	β (°)[g,h]	ɣ (°)[g,h]
Hist		1.8(1)	0.72(2)	16(5)	–	–	–	–	–
Ambr		5.6(2)	0.82(2)	74(25)	–	–	–	–	–
Diph		4.6(2)	0.16(4)	50(50)	20(50)	0.48(25)	0(90)	0(45)	0(45)
Isox		5.7(2)	0.27(3)	120(50)	50(50)	0.5(3)	0(90)	0(45)	0(45)
Ceti	Site 1	7.3(1)	0.65(5)	120(10)	–	–	–	–	–
	Site 2	4.0(5)	0.90(5)	50(10)	–	–	–	–	–

[a]The experimental uncertainty in the last digit(s) for each value is indicated in parentheses.
[b]$C_Q = eQV_{33}/h$; [c]$\eta_Q = (V_{11} - V_{22})/V_{33}$; [d]$\delta_{iso} = (\delta_{11} + \delta_{22} + \delta_{33})/3$; [e]$\Omega = \delta_{11} - \delta_{33}$; [f]$\kappa = 3(\delta_{22} - \delta_{iso})/\Omega$. [g]The Euler angles, α, β, and ɣ, define the relative orientation of the CS and EFG tensors. [h]Accurate determination of the CSA parameters and Euler angles is not possible without spectra acquired at a second field strength. For diph and isox, CSA parameters were used based on those previously reported.[21]

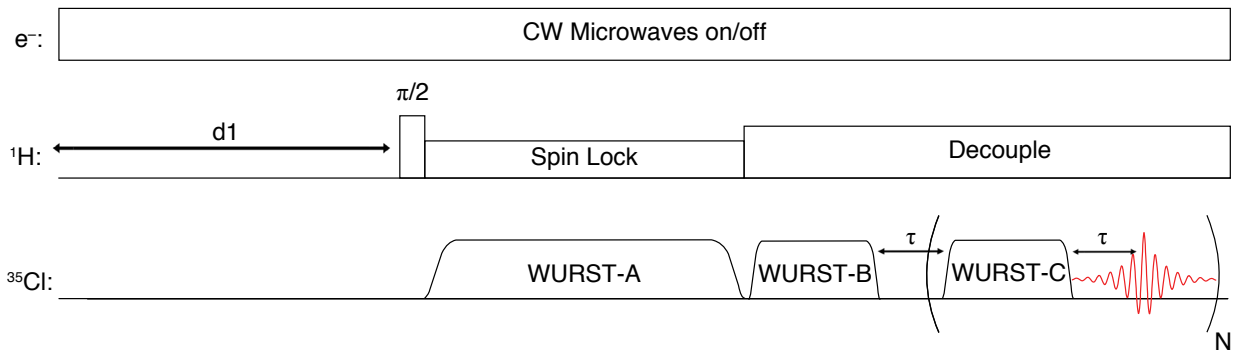

Figure S1. ^{1}H-^{35}Cl BCP pulse sequence used for the DNP-enhanced ^{35}Cl SSNMR experiments. For start-stop MAS experiments, the sample was rotated during the recycle delay (d1).

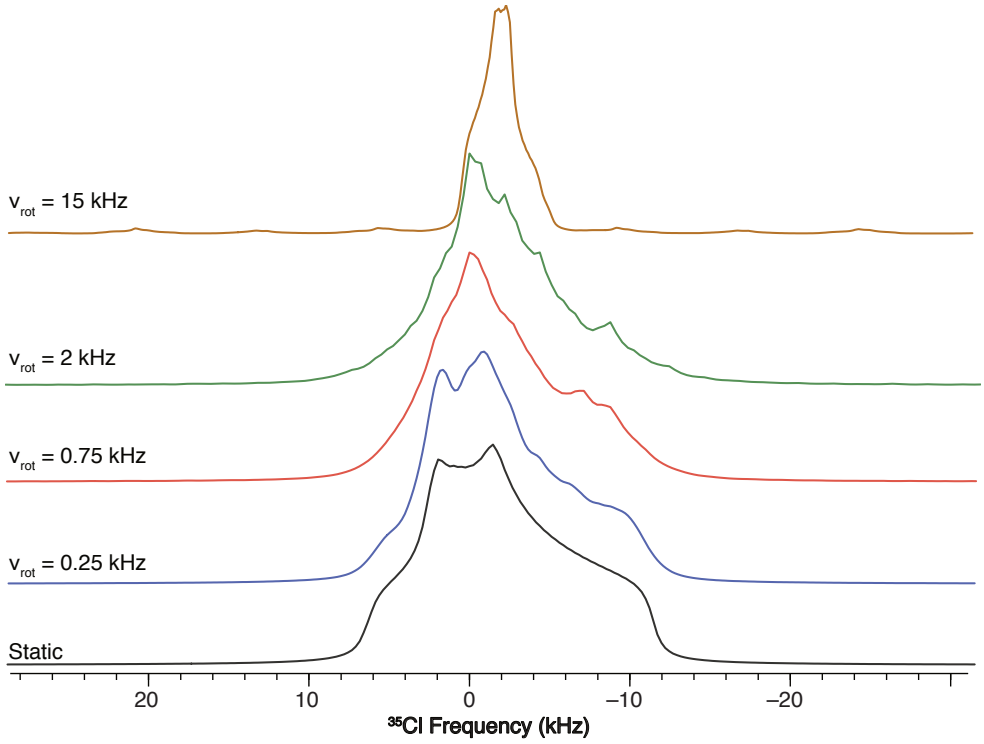

Figure S2. Simulated ^{35}Cl SSNMR spectra of **hist** under MAS at various spinning speeds.

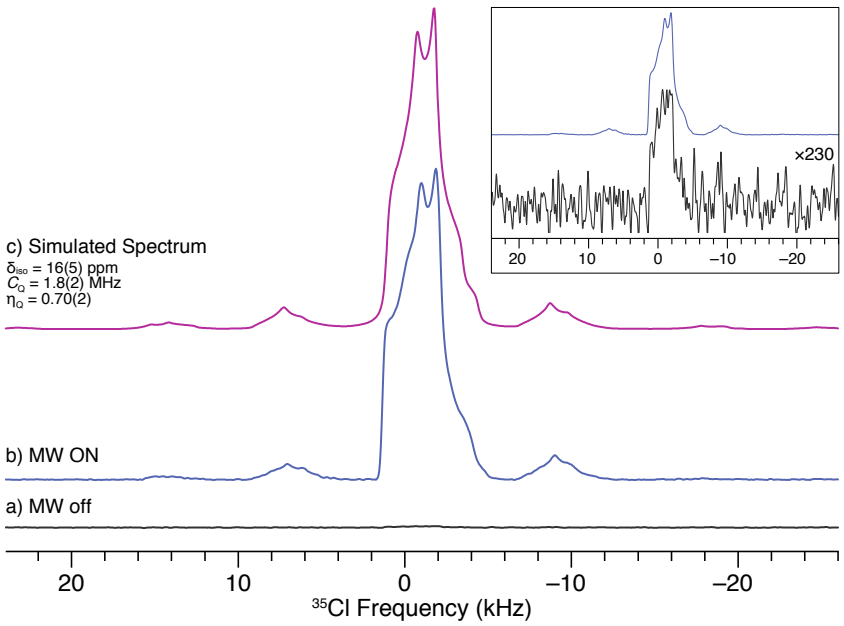

Figure S3. ^{1}H-^{35}Cl CP-echo MAS (ν_{rot} = 8 kHz) SSNMR spectra of **hist** acquired with a) microwaves off, and b) microwaves on. c) shows an analytical simulation of the spectra and the parameters used to generate the simulated spectrum. The inset contains the experimental spectra scaled to the same maximum intensity.

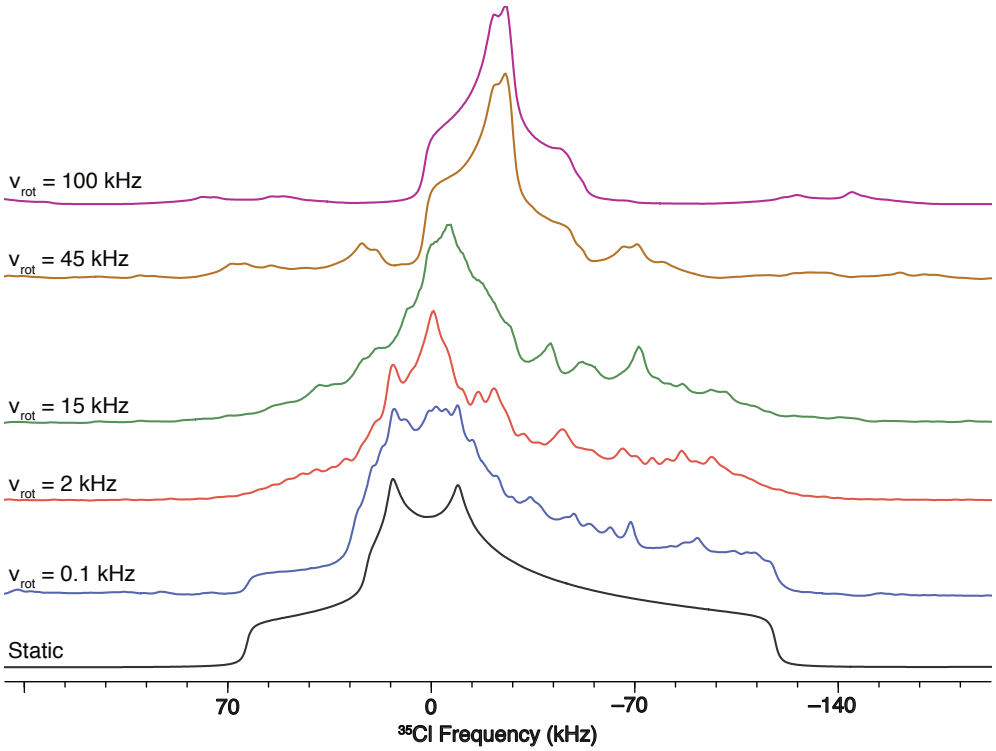

Figure S4. Simulated ^{35}Cl SSNMR spectra of **ambr** under MAS at various spinning speeds.

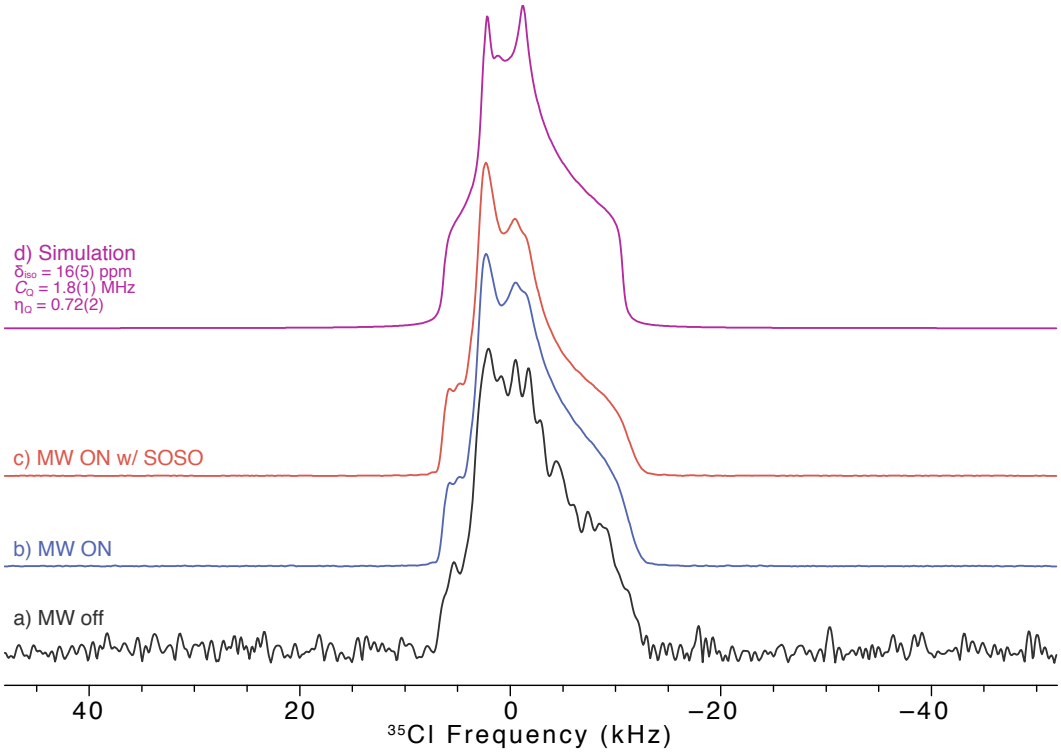

Figure S5. ^{1}H-^{35}Cl CP SSNMR spectra of **hist** (a-c) and the corresponding analytical simulation (d). The parameters used to generate the simulated spectrum are shown in the figure.

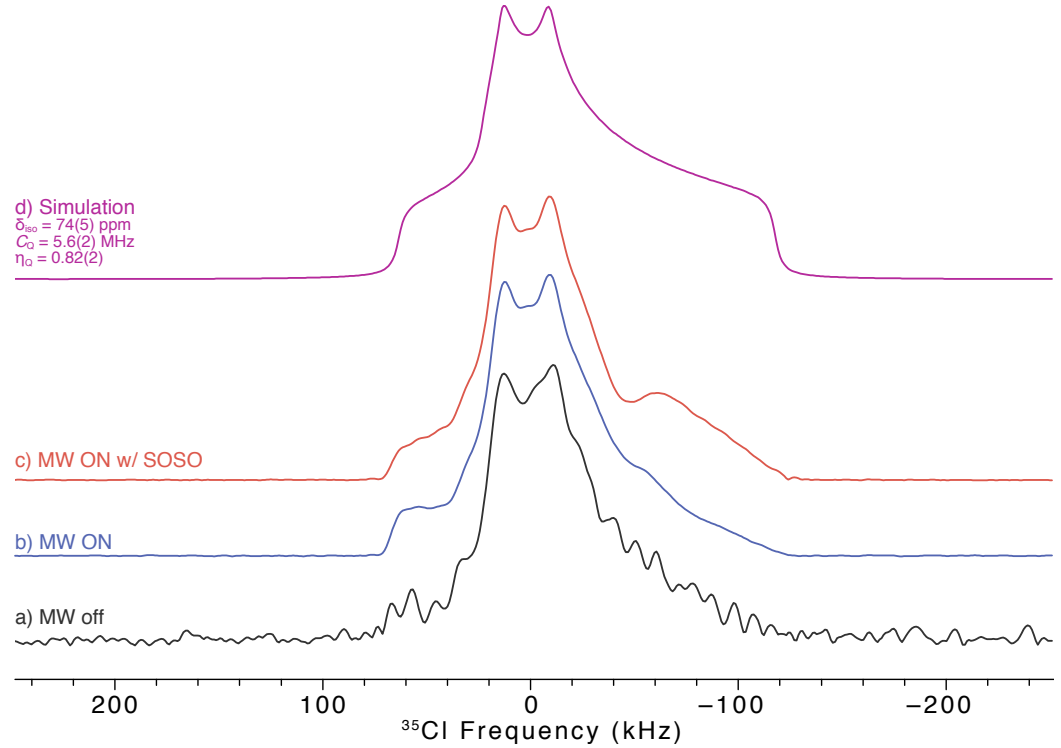

Figure S6. ^{1}H-^{35}Cl BCP SSNMR spectra of **ambr** (a-c) and the corresponding analytical simulation (d). Parameters used to generate the simulated spectrum are listed in the figure.

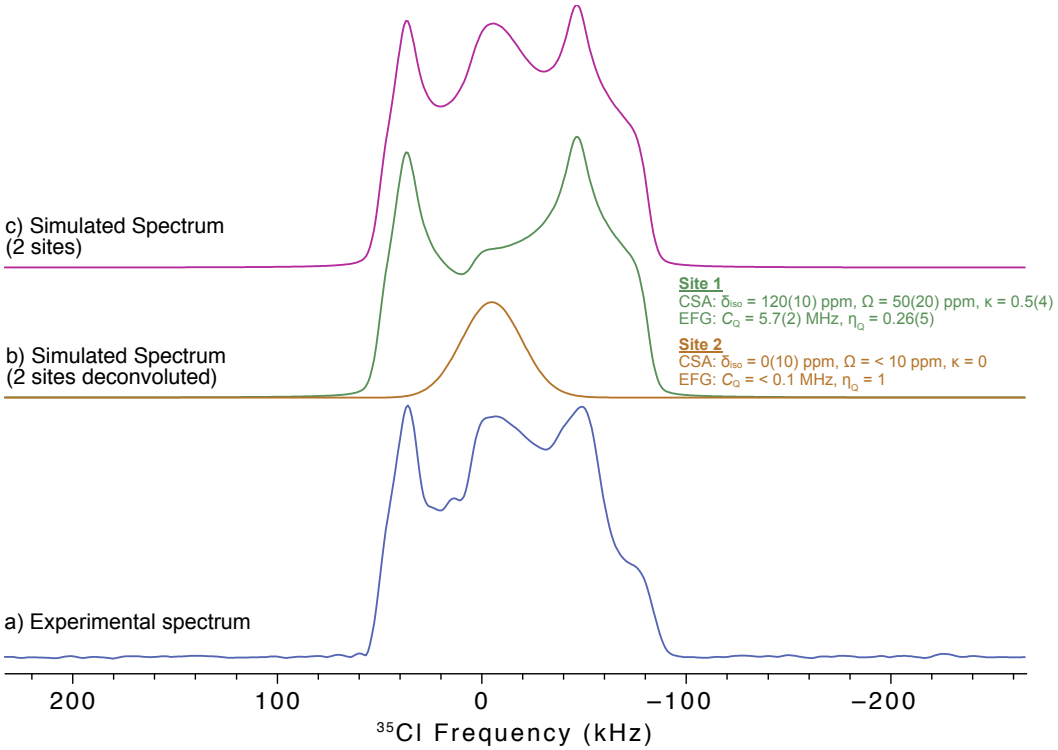

Figure S7. ^{1}H-^{35}Cl BCP SSNMR spectrum of **isox** (a) and the corresponding two-site analytical simulation (b-c). Parameters used to generate the simulated spectra are listed in the figure.

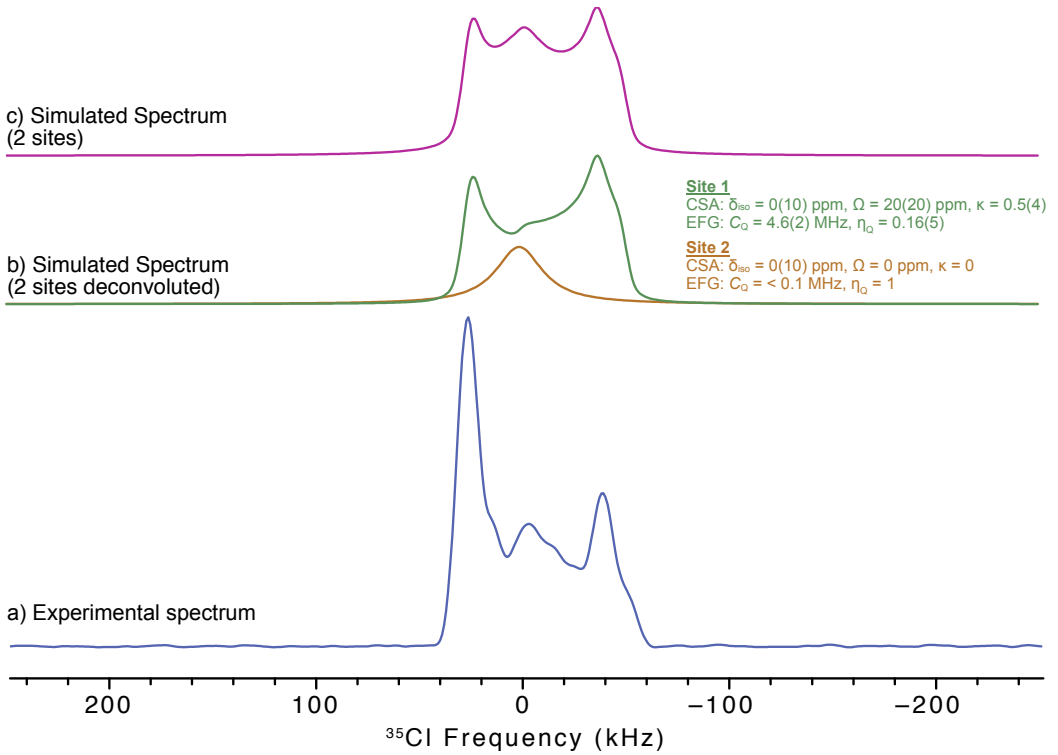

Figure S8. ^{1}H-^{35}Cl BCP SSNMR spectrum of **diph** (a) and the corresponding two-site analytical simulation (b-c). Parameters used to generate the simulated spectra are listed in the figure.

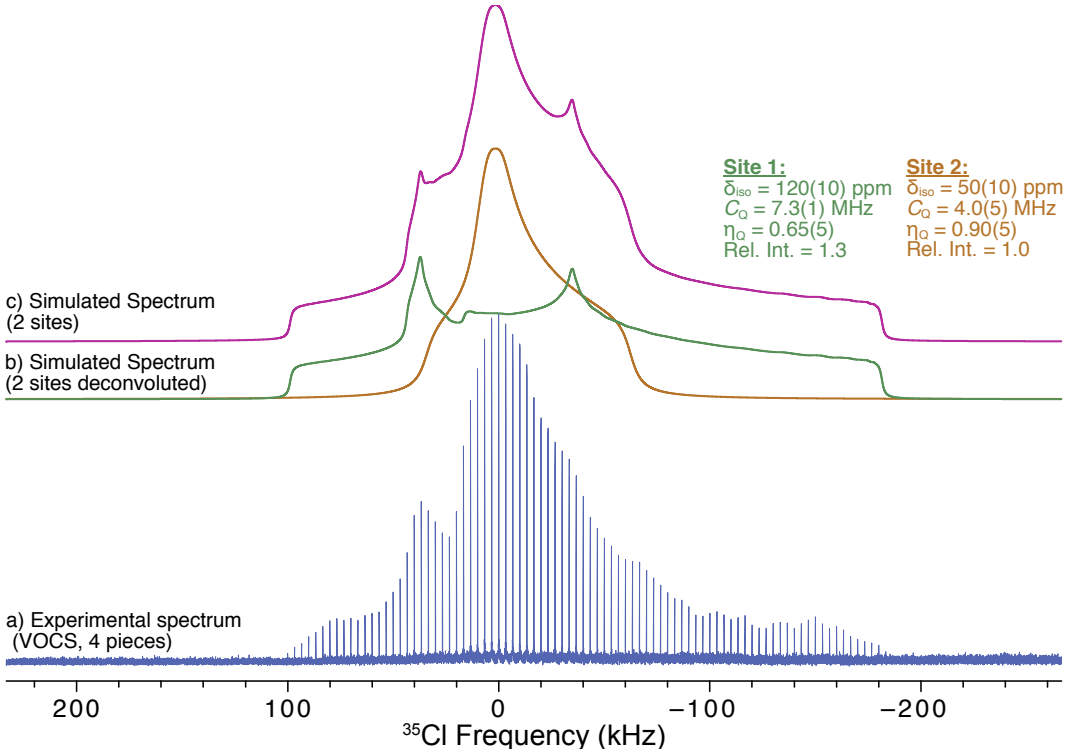

Figure S9. a) Experimental ^{1}H-^{35}Cl BCP SSNMR spectrum of **ceti** acquired with VOCS acquisition. Four sub-spectra were coadded together to produce the final spectrum. b) and c) show the 2-site simulation of the pattern as a deconvolution and combined spectrum, respectively. The quadrupolar parameters associated with this simulation are shown on the right of the figure.

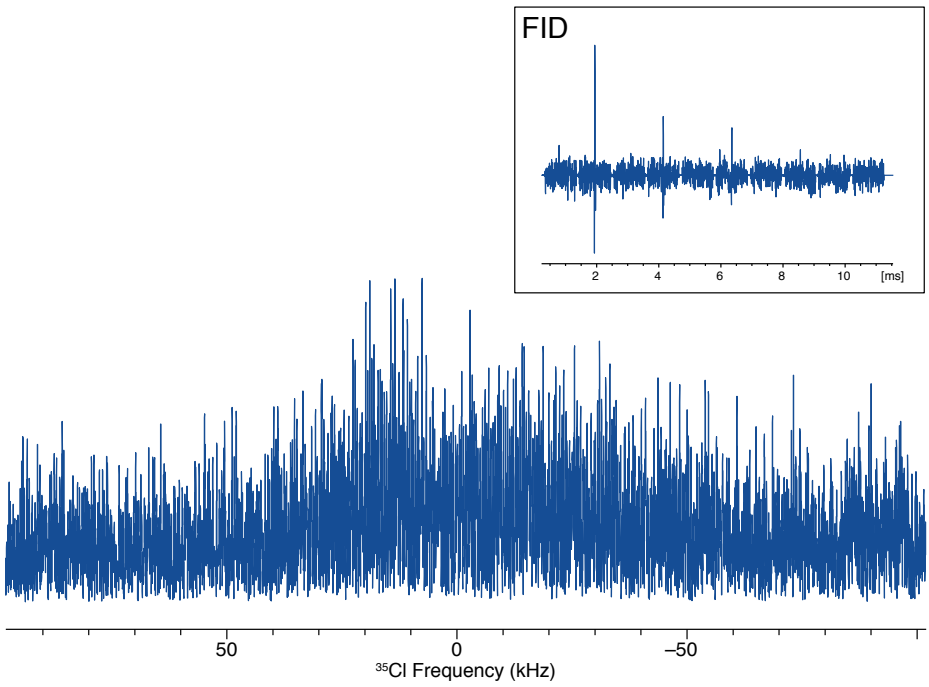

Figure S10. ^{1}H-^{35}Cl BCP-WCPMG spectrum of **ambr** acquired with 700 mb bearing gas flow and no drive gas flow (~ 4 Hz spinning detected). The FID for this spectrum (inset) has several echoes that are not properly refocused due to the spinning.

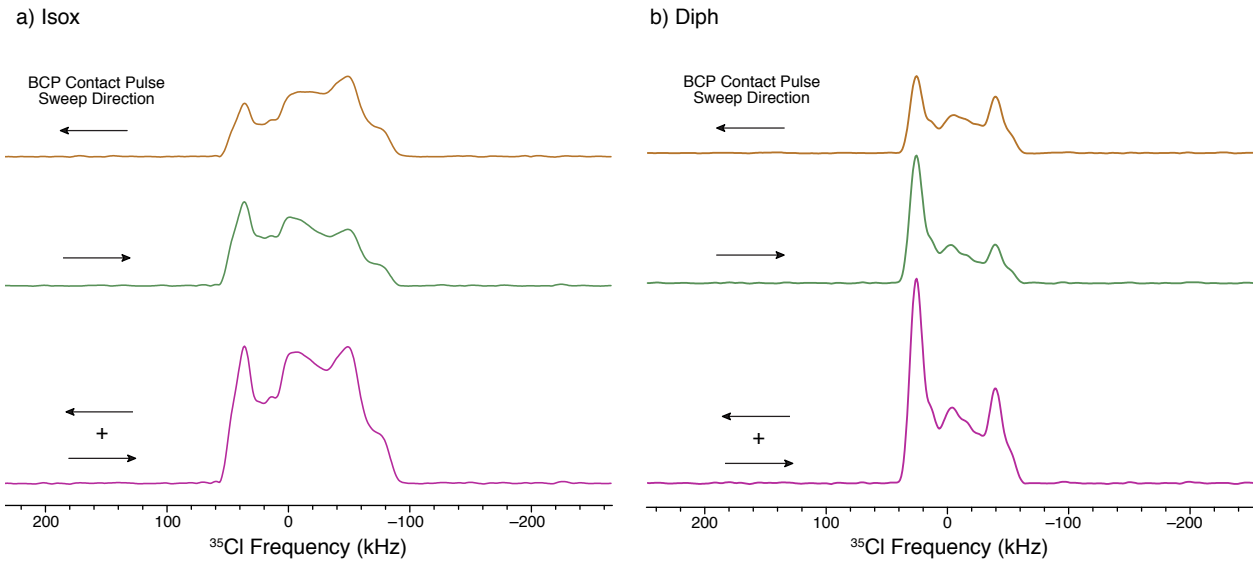

Figure S11. ^{1}H-^{35}Cl BCP SSNMR spectra of a) isox and b) diph acquired with MW on. As shown in the figure, the sweep direction of the BCP contact pulse has a large effect on the shape of the pattern. This effect may result from relaxation processes [*i.e.*, $T_1\rho(^{1}H)$] occurring over the course of the swept pulse that cause differences in CP efficiency. The true lineshape is obtained by combining two sub-spectra acquired when sweeping in opposite directions (purple).

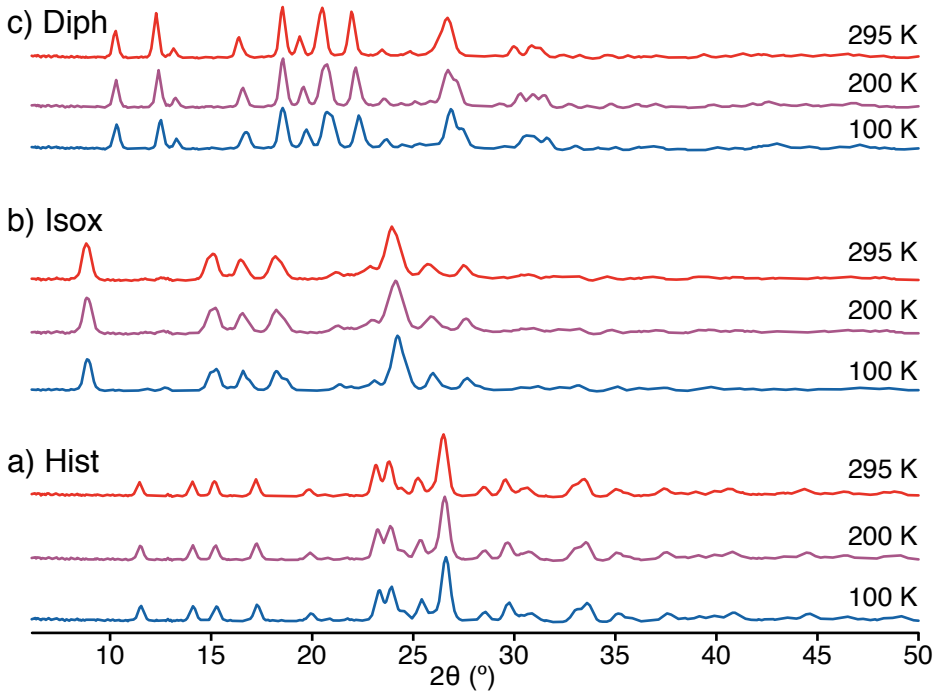

Figure S12. VT-pXRD diffraction patterns of a) **hist**, b) **isox**, and c) **diph** acquired at three temperatures: 295 K, 200 K, and 100 K. The patterns indicate that the crystalline structure of each material remains unchanged with cooling to 100 K.

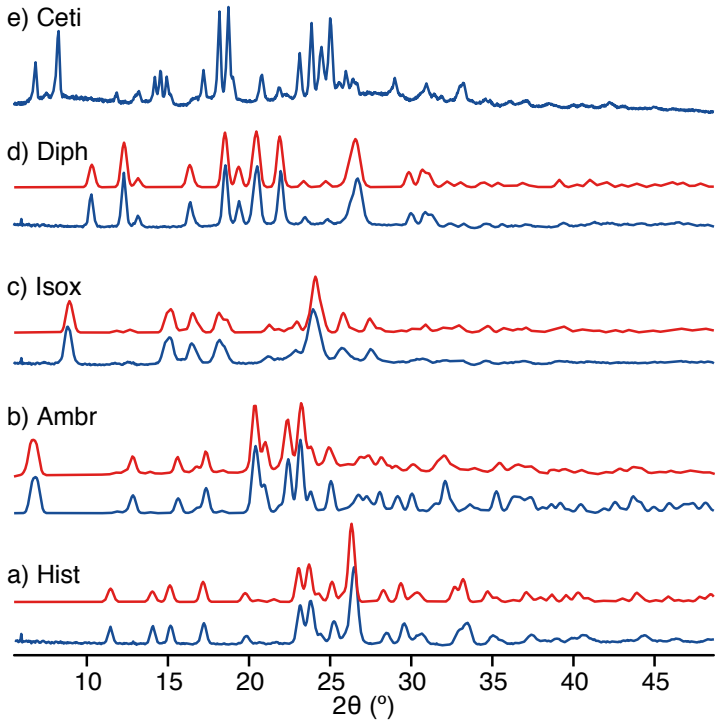

Figure S13. pXRD patterns of as received a) **hist**, b) **ambr**, c) **isox**, d) **diph,** and e) **ceti** obtained experimentally at 298 K (blue) or simulated using published crystal structures[81–84] (red). No simulated pattern is available for **ceti** due to the lack of a published crystal structure.

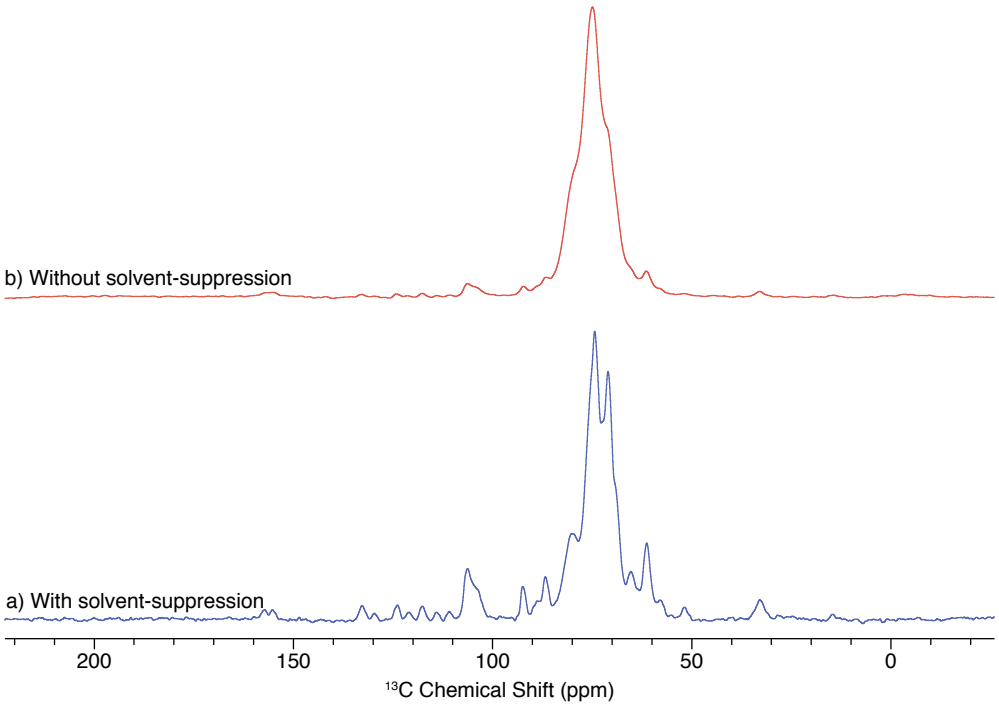

Figure S14. ^{1}H-^{13}C CP/MAS (ν_{rot} = 9 kHz) spectra of the dosage form of **isox** acquired a) with a 10 ms spin-echo added to the pulse sequence for solvent suppression, and b) without the use of a spin-echo.

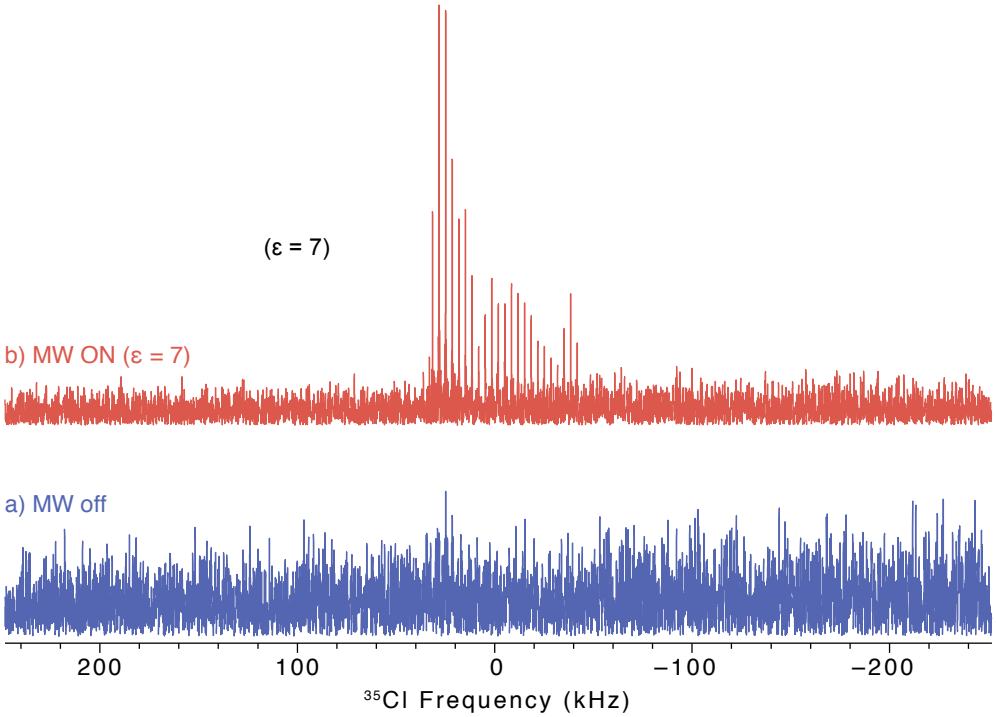

Figure S15. ^{1}H-^{35}Cl BCP spectra of diph acquired with a) microwaves off and b) microwaves on used to measure the DNP enhancement. Both spectra were acquired with one BCP sweep direction and a Fourier transform was applied directly to the CPMG echo train (i.e., without coadding the echoes).